Reaction of $[P_2N_2]Ta{=}CH_2(Me)$ with Ethylene: Synthesis of $[P_2N_2]Ta(C_2H_4)Et$, a Neutral Species with a β-Agostic Ethyl Group in Equilibrium with an α-Agostic Ethyl Group ($[P_2N_2]$ = $PhP(CH_2SiMe_2NSiMe_2CH_2)_2PPh$)

Michael D. Fryzuk,* Samuel A. Johnson, and Steven J. Rettig[†]

Contribution from the Department of Chemistry, University of British Columbia, 2036 Main Mall, Vancouver, B.C., Canada V6T 1Z1

Received June 16, 2000

Abstract: The photolysis of $[P_2N_2]TaMe_3$ ($[P_2N_2]$ = $PhP(CH_2SiMe_2NSiMe_2CH_2)_2PPh$) produces $[P_2N_2]Ta{=}CH_2(Me)$ as the major product. The thermally unstable methylidene complex decomposes in solution in the absence of trapping agents to unidentified products. However, in the presence of ethylene $[P_2N_2]Ta{=}CH_2(Me)$ is slowly converted to $[P_2N_2]Ta(C_2H_4)Et$, with $[P_2N_2]Ta(C_2H_4)Me$ observed as a minor product. A mechanistic study suggests that the formation of $[P_2N_2]Ta(C_2H_4)Et$ results from the trapping of $[P_2N_2]TaEt$, formed by the migratory insertion of the methylene moiety into the tantalum−methyl bond. The minor product, $[P_2N_2]Ta(C_2H_4)Me$, forms from the decomposition of a tantalacyclobutane resulting from the addition of ethylene to $[P_2N_2]Ta{=}CH_2(Me)$ and is accompanied by the production of an equivalent of propylene. Pure $[P_2N_2]Ta(C_2H_4)Et$ can be synthesized by hydrogenation of $[P_2N_2]TaMe_3$ in the presence of PMe_3, followed by the reaction of ethylene with the resulting trihydride. Crystallographic and NMR data indicate the presence of a β-agostic interaction between the ethyl group and tantalum center in $[P_2N_2]Ta(C_2H_4)Et$. Partially deuterated analogues of $[P_2N_2]Ta(C_2H_4)Et$ show a large isotopic perturbation of resonance for both the β-protons and the α-protons of the ethyl group, indicative of an equilibrium between a β-agostic and an α-agostic interaction for the ethyl group in solution. An EXSY spectrum demonstrates that an additional fluxional process occurs that exchanges all of the ^1H environments of the ethyl and ethylene ligands. The mechanism of this exchange is believed to involve the direct transfer of the β-agostic hydrogen atom from the ethyl group to the ethylene ligand, via the so-called β-hydrogen transfer process.

Introduction

Agostic interactions involving C−H bonds are more than just a structural curiosity; they have been shown to be important in C−H activation processes[1,2] as well as in olefin polymerization. With respect to polymerization, β-agostic interactions have been implicated in the resting state of many early and late metal polymerization catalysts,[3−6] and thus may be relevant to catalyst activity and polymer molecular weights.[7−14] Similarly, α-agostic interactions have been examined for their ability to direct olefin insertion.[11]

There are numerous examples of β-agostic interactions, where a β-C−H bond of an alkyl ligand interacts with the metal center providing a 3-center, 2-electron bonding interaction.[4,15] For the simplest alkyl group in which this interaction is possible, the ethyl group, β-agostic interactions are usually associated with coordinatively unsaturated and cationic complexes.[16−19] For neutral complexes, a few β-agostic ethyl groups have been postulated on the basis of NMR, EPR, and IR data;[20−22]

[†] Professional Officer: UBC X-ray Structural Laboratory (Deceased October 27, 1998).

(1) Ginzburg, A. G. *Russ. Chem. Rev.* **1988**, *57*, 1175.
(2) Gleiter, R.; Hyla-Kryspin, I.; Niu, S. Q.; Erker, G. *Organometallics* **1993**, *12*, 3828.
(3) Brookhart, M.; Green, M. L. H. *J. Organomet. Chem.* **1983**, *250*, 395.
(4) Brookhart, M.; Green, M. L. H.; Wong, L. L. *Prog. Inorg. Chem.* **1988**, *36*, 1.
(5) Brintzinger, H. H.; Fischer, D.; Mülhaupt, R.; Rieger, B.; Waymouth, R. M. *Angew. Chem., Int. Ed. Engl.* **1995**, *34*, 1143.
(6) Woo, T. K.; Margl, P. M.; Lohrenz, J. C. W.; Blöchl, P. E.; Ziegler, T. *J. Am. Chem. Soc.* **1996**, *118*, 13021.
(7) Schmidt, G. F.; Brookhart, M. *J. Am. Chem. Soc.* **1985**, *107*, 1443.
(8) Burger, B. J.; Thompson, M. E.; Cotter, W. D.; Bercaw, J. E. *J. Am. Chem. Soc.* **1990**, *112*, 1566.
(9) Resconi, L.; Piemontesi, F.; Franciscono, G.; Abis, L.; Fiorani, T. *J. Am. Chem. Soc.* **1992**, *114*, 1025.
(10) Guo, Z.; Swenson, D. C.; Jordan, R. F. *Organometallics* **1994**, *13*, 1424.
(11) Grubbs, R. H.; Coates, G. W. *Acc. Chem. Res.* **1996**, *29*, 85.
(12) Prosenc, M. H.; Janiak, C.; Brintzinger, H. H. *Organometallics* **1992**, *11*, 4036.
(13) Röll, W.; Brintzinger, H. H.; Rieger, B.; Zolk, R. *Angew. Chem., Int. Ed. Engl.* **1990**, *29*, 279.
(14) Cavallo, L.; Guerra, G.; Vacatello, M.; Corradini, P. *Macromolecules* **1991**, *24*, 1784.
(15) Crabtree, R. H.; Hamilton, D. G. *Adv. Organomet. Chem.* **1988**, *28*, 299.
(16) Jordan, R. F.; Bradley, P. K.; Baenziger, N. C.; LaPointe, R. E. *J. Am. Chem. Soc.* **1990**, *112*, 1289.
(17) Mole, L.; Spencer, J. L.; Carr, N.; Orpen, A. G. *Organometallics* **1991**, *10*, 49.
(18) Conroy-Lewis, F. M.; Mole, L.; Redhouse, A. D.; Lister, S. A.; Spencer, J. L. *J. Chem. Soc., Chem. Commun.* **1991**, 1601.
(19) Cracknell, R. B.; Orpen, A. G.; Spencer, J. L. *J. Chem. Soc., Chem. Commun.* **1984**, 326.
(20) Fellmann, J. D.; Schrock, R. R.; Traficante, D. D. *Organometallics* **1982**, *1*, 481.
(21) Thompson, M. E.; Baxter, S. M.; Bulls, A. R.; Burger, B. J.; Nolan, M. C.; Santasiero, B. D.; Shaefer, W. P.; Bercaw, J. E. *J. Am. Chem. Soc.* **1987**, *109*, 203.
(22) Lukens, W. W. J.; Smith, M. R. I.; Andersen, R. A. *J. Am. Chem. Soc.* **1996**, *118*, 1719.

10.1021/ja0021621 CCC: $20.00
Published on Web 01/31/2001

however, the only structurally characterized example of a neutral complex with a β-agostic ethyl group is the 12-electron species TiCl$_3$(dmpe)Et,[23,24] and the bonding in this species continues to be the subject of theoretical studies.[25−29] There are also a number of reports of α-agostic interactions,[4,11] although for the ethyl group this interaction is believed to be preferred only when steric bulk disfavors a β-agostic interaction.[30]

We have recently reported the synthesis of a methylidene complex of tantalum, [P$_2$N$_2$]Ta=CH$_2$(Me)[31] (where [P$_2$N$_2$] = PhP(CH$_2$SiMe$_2$NSiMe$_2$CH$_2$)$_2$PPh). While isolable, this compound is not stable when stored in solution at room temperature. In analogy to the decomposition of the first isolated methylidene complex, (η^5-C$_5$H$_5$)$_2$Ta=CH$_2$(Me),[32] an 18-electron species, we expected the decomposition of the less electronically saturated [P$_2$N$_2$]Ta=CH$_2$(Me) in the presence of ethylene gas would yield [P$_2$N$_2$]Ta(C$_2$H$_4$)Me. Instead, the major product is the ethylene ethyl compound [P$_2$N$_2$]Ta(C$_2$H$_4$)Et, which features a β-agostic interaction in the solid-state structure despite the fact that this species is neither cationic nor exceptionally coordinatively unsaturated. Furthermore, the β-agostic interaction appears to be in rapid equilibrium with an α-agostic structure in solution. Herein we report a mechanistic study of the reaction of [P$_2$N$_2$]-Ta=CH$_2$(Me) with ethylene and a description of the β-agostic interaction and associated fluxional processes observed in [P$_2$N$_2$]-Ta(C$_2$H$_4$)Et.

Results and Discussion

We have previously reported the preparation of [P$_2$N$_2$]TaMe$_3$ and its hydrogenation to yield a dinuclear Ta(IV) hydride.[31,33] The macrocyclic ancillary ligand [P$_2$N$_2$][34] is a flexible framework of two amide and two phosphine donors that has been shown to stabilize complexes of the early transition metals,[35−37] the main group elements,[38] and the lanthanides[39] in a variety of geometries.

Photolysis of [P$_2$N$_2$]TaMe$_3$ generates the isolable methylidene complex, [P$_2$N$_2$]Ta=CH$_2$(Me),[31] which is reasonably stable in the solid state; however, in solution at room temperature this derivative decomposes to NMR inactive unidentified products over the course of about one month. In an attempt to elucidate the mechanisms and chemistry involved in this thermal decomposition, we examined the decomposition of [P$_2$N$_2$]Ta=CH$_2$-(Me) in the presence of three potential trapping agents: ethylene, trimethylphospine, and propylene. Of these, ethylene alone proved successful in allowing the characterization and isolation of products of the methylidene complex's decomposition.

Photolysis of [P$_2$N$_2$]TaMe$_3$ in the Presence of C$_2$H$_4$. As previously reported, a solution of [P$_2$N$_2$]TaMe$_3$ gradually darkens as it is photolyzed; uncharacterized paramagnetic impurities are formed, likely from the photolysis of the desired product, [P$_2$N$_2$]Ta=CH$_2$(Me).[31] The photolysis of [P$_2$N$_2$]TaMe$_3$ in the presence of ethylene is visibly different, as the solution does not darken even with long photolysis times, and a light orange/red solution results. The initial product of the photolysis in the presence of ethylene remains the methylidene [P$_2$N$_2$]Ta=CH$_2$(Me), and both the ^{1}H and ^{31}P{^{1}H} NMR spectra show it to be the major product; however, performing this reaction in a NMR tube containing an internal concentration standard demonstrates that a considerable amount of paramagnetic, NMR-inactive side products must also exist. When the photolysis time is sufficiently long for all of the [P$_2$N$_2$]TaMe$_3$ starting material to react, only a ~50% yield of [P$_2$N$_2$]Ta=CH$_2$(Me) is obtained (relative to internal ferrocene by ^{1}H NMR spectroscopy), although this value varies from 40 to 60% depending on the exact conditions employed.

Reaction of [P$_2$N$_2$]Ta=CH$_2$(Me) with C$_2$H$_4$. Although ethylene appears to react immediately with the dark paramagnetic impurities produced in the photolysis of [P$_2$N$_2$]TaMe$_3$ as evidenced by the difference in the color of the solution after photolysis, ethylene also reacts with the methylidene complex [P$_2$N$_2$]Ta=CH$_2$(Me). This latter reaction is slow, comparable in rate to the thermal decomposition of [P$_2$N$_2$]Ta=CH$_2$(Me). Monitoring the reaction by ^{1}H and ^{31}P{^{1}H} NMR spectroscopies over the course of two weeks, two new products appeared, and no [P$_2$N$_2$]Ta=CH$_2$(Me) remained. The major product was identified by a combination of ^{1}H, ^{13}C{^{1}H}, and ^{31}P{^{1}H} NMR spectroscopies as the ethylene−ethyl complex, [P$_2$N$_2$]Ta(C$_2$H$_4$)-Et (**1**), and the minor product as the ethylene−methyl derivative, [P$_2$N$_2$]Ta(C$_2$H$_4$)Me (**2**). The total concentration of complexes **1** and **2** was equal to that of the original [P$_2$N$_2$]Ta=CH$_2$(Me) by comparison to an internal concentration standard, which indicates that the source of the NMR-active products was [P$_2$N$_2$]-Ta=CH$_2$(Me) and not the NMR-inactive products. The dark red NMR-inactive products resulting from the reaction with ethylene have vastly different solubilities than complexes **1** and **2** and could be removed by washing with hexanes. NMR spectroscopic analyses (^{1}H and ^{13}C{^{1}H}) and GC-MS showed propylene and 1-butene to be the organic products of this reaction. The tantalum-containing reaction products are depicted in Scheme 1.

Alternate Synthesis and Structure of [P$_2$N$_2$]Ta(C$_2$H$_4$)Et (1). Complexes **1** and **2** proved difficult to separate by fractional crystallization. Both are soluble in aromatic solvents and have poor solubility in hexanes. Attempts to isolate complex **1** by exposing a benzene solution of these two complexes to air with the intention that the less sterically crowded methyl complex **2** might be more reactive led to the surprising revelation that both these complexes are air stable. A benzene solution of **1** and **2** showed no signs of decomposition of either complex after 4 h of exposure to air. Due to the lack of success in separating complex **1** from complex **2**, an alternate route to **1** was sought, to determine its structure in the solid state by X-ray crystallography.

(23) Dawoodi, Z.; Green, M. L. H.; Mtetwa, V. S. B.; Prout, K. *J. Chem. Soc., Chem. Commun.* **1982**, 802.
(24) Dawoodi, Z.; Green, M. L. H.; Mtetwa, V. S. B.; Prout, K.; Schultz, A. J.; Williams, J. M.; Koetzle, T. F. *J. Chem. Soc., Dalton Trans.* **1986**, 1629.
(25) Haaland, A.; Scherer, W.; Ruud, K.; McGrady, G. S.; Downs, A. J.; Swang, O. *J. Am. Chem. Soc.* **1998**, *120*, 3762.
(26) Scherer, W.; Priermeier, T.; Haaland, A.; Volden, H. V.; McGrady, G. S.; Downs, A. J.; Boese, R.; Blaser, D. *Organometallics* **1998**, *17*, 4406.
(27) McGrady, G. S.; Downs, A. J. *Coord. Chem. Rev.* **2000**, *197*, 95.
(28) Cotton, F. A.; Petrukhina, M. A. *Inorg. Chem. Commun.* **1998**, *1*, 195.
(29) Munakata, H.; Ebisawa, Y.; Takashima, Y.; Wrinn, M. C.; Scheiner, A. C.; Newsam, J. M. *Catal. Today* **1995**, *23*, 403.
(30) Etienne, M.; Mathieu, R.; Donnadieu, B. *J. Am. Chem. Soc.* **1997**, *119*, 3218.
(31) Fryzuk, M. D.; Johnson, S. A.; Rettig, S. J. *Organometallics* **1999**, *18*, 4059.
(32) Schrock, R. R. *J. Am. Chem. Soc.* **1975**, *97*, 6577.
(33) Fryzuk, M. D.; Johnson, S. A.; Rettig, S. J. *Organometallics* **2000**, *19*, 3931.
(34) Fryzuk, M. D.; Love, J. B.; Rettig, S. J. *J. Chem. Soc., Chem. Commun.* **1996**, 2783.
(35) Basch, H.; Musaev, D. G.; Morokuma, K.; Fryzuk, M. D.; Love, J. B.; Seidel, W. W.; Albinati, A.; Koetzle, T. F.; Klooster, W. T.; Mason, S. A.; Eckert, J. *J. Am. Chem. Soc.* **1999**, *121*, 523.
(36) Fryzuk, M. D.; Love, J. B.; Rettig, S. J.; Young, V. G. *Science* **1997**, *275*, 1445.
(37) Fryzuk, M. D.; Love, J. B.; Rettig, S. J. *Organometallics* **1998**, *17*, 846.
(38) Fryzuk, M. D.; Giesbrecht, G. R.; Rettig, S. J. *Inorg. Chem.* **1998**, *37*, 6928.
(39) Fryzuk, M. D.; Love, J. B.; Rettig, S. J. *J. Am. Chem. Soc.* **1997**, *119*, 9071.

Scheme 1

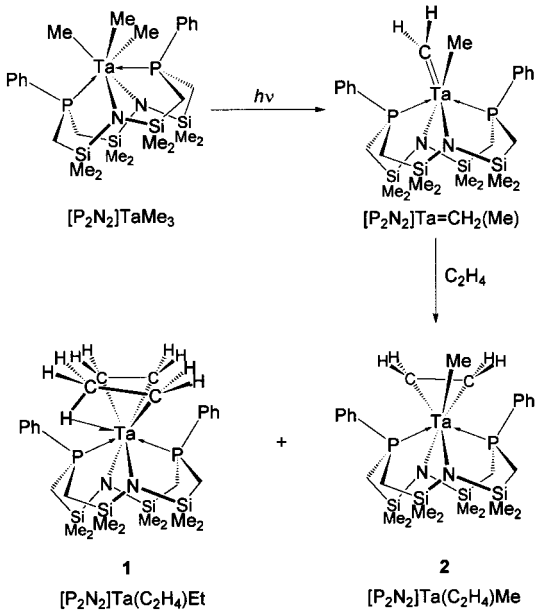

A viable route to a pure **1** might be through the reaction of ethylene with a Ta(V) hydride, such as $[P_2N_2]TaH_3$. Attempts to prepare this trihydride via the hydrogenation of $[P_2N_2]TaMe_3$ led only to the dinuclear hydride $([P_2N_2]Ta)_2(\mu\text{-}H)_4$,[33] which does not react with ethylene. The hydrogenation of $[P_2N_2]TaMe_3$ in the presence of ethylene resulted in catalytic hydrogenation of the ethylene to ethane and the previously characterized monohydride $[P_2N_2]TaMe_2H$.[33] It proved possible to generate the mononuclear trihydride $[P_2N_2]TaH_3(PMe_3)$, **3**, by the hydrogenation of $[P_2N_2]TaMe_3$ in the presence of excess PMe_3. Complex **1** was then readily synthesized in an overall yield of 95% by the reaction of $[P_2N_2]TaH_3(PMe_3)$ with ethylene, as shown in Scheme 2.

The solid-state molecular structure of **1** is shown in Figure 1, and crystallographic data are given in Table 1. The nine hydrogen atoms associated with the ethylene and ethyl ligands were identified in an electron density difference map, and their locations were refined. Immediately evident from this structure is the β-agostic interaction. The agostic Ta(1)−C(26) distance of 2.498(4) Å is only ~0.25 Å longer than the σ-bound Ta(1)−C(25) distance of 2.251(3) Å. The ethylene moiety also has two significantly different Ta−C bond lengths, where the longer Ta−C bond is with the carbon diagonally opposing the agostically bound β-carbon of the ethyl group; the Ta(1)−C(27) distance is 2.251(3) Å, whereas the Ta(1)−C(28) is 2.362(4) Å. A single hydrogen atom attached to the β-carbon of the ethyl group is directed toward the metal with a Ta(1)−H(45) distance of 2.07(4) Å. The back-bonding to the ethylene moiety is significant enough that it is probably best described as a metallacyclopropane. The C(25)−C(26) bond length in the ethyl ligand and the C(27)−C(28) bond length in the ethylene ligand are identical at 1.449(5) Å. These distances are both slightly shorter than typical carbon−carbon single bonds, but much longer than a carbon−carbon double bond. If one considers the η^2-ethylene and η^2-ethyl groups to each occupy a single coordination site, the overall geometry of complex **1** is best described as distorted octahedral. As is common for complexes of the $[P_2N_2]$ ligand, the phosphorus donors are approximately trans with a P(1)−Ta(1)−P(2) angle of 160.18(3)°, and the nitrogen donors are closer to a cis orientation with a N(1)−Ta(1)−N(2) angle of 97.02(9)°. The "twist" of the amide donors that has been described for other complexes of the $[P_2N_2]$ ligand, including those containing Ta, is quite small in **1**.[31,33] The twist can be quantified by the difference between the P(1)−Ta(1)−N(1)−Si(4) and P(2)−Ta(1)−N(1)−Si(1) dihedral angles, which is 19.2(3)°. Compound **1** is a 16-electron complex if one includes the donation of electrons from the agostic interaction, but does not consider possible π-donation from the amide lone pairs. As has been shown before,[31,33] without a twist in the $[P_2N_2]$ ligand framework only one linear combination of the two amido-based lone pair p-orbitals has overlap with an unoccupied metal orbital of appropriate symmetry, and therefore compound **1** can be considered an 18-electron species.

NMR Spectral Data for $[P_2N_2]Ta(C_2H_4)Et$. Does the ethyl group maintain the β-agostic interaction in solution? The resonances for the ethyl group in **1** are prominent in the $^1H\{^{31}P\}$ NMR spectrum, with a quartet for the α-hydrogens of the ethyl group at δ −1.27 and a triplet for the β-protons at δ −0.51. Simulation of the phosphorus-31 coupled ^1H NMR spectrum of the tantalum ethyl group provided the coupling constants of the α and β hydrogens to phosphorus of $^3J_{PH}$ = 3.1 Hz and J_{PH} = 4.4 Hz, respectively. The larger coupling to the β-hydrogens of the ethyl group (compared to the α) and the low frequency observed for these protons provide strong evidence that there is an agostic interaction of a β-C−H bond with the tantalum metal center in solution. In comparison, for the related 18-electron species $(\eta^5\text{-}C_5H_5)_2Nb(C_2H_4)Et$,[40] in which there is no agostic interaction, the β-CH_3 resonance appears at δ 1.83; in a less electronically saturated ethylniobium species with an α-agostic interaction, the β-CH_3 group appears at δ 1.15.[30] Both of these groups have chemical shifts in the same region as ethyl groups in organic compounds. The single chemical environment for the β-hydrogens of the ethyl group in **1** indicates that there is rapid rotation of the terminal CH_3 group, so that the observed 4.4 Hz coupling is an average of the P−H couplings arising from the single agostic hydrogen (quasi two-bond coupling) and the two terminal hydrogens (four-bond coupling). If it is assumed that the coupling of phosphorus-31 to the more distant terminal β-hydrogens is much smaller, the actual coupling of phosphorus-31 to the β-agostic hydrogen can be estimated as at least three times this 4.4 Hz value, or 13.2 Hz; however, this approximation assumes that the β-agostic interaction is maintained at all times in solution. Likewise, the chemical shift for the β-CH_3 group (δ −0.51) is an average of the two terminal and one agostic β-hydrogens, although between 180 and 350 K only one environment is observed for the β-CH_3 group in the 500 MHz ^1H NMR spectrum.

On the NMR time-scale complex **1** appears to have a mirror plane of symmetry such that the two phosphorus donors are equivalent but the two amides are not. Thus, two signals are evident in the ^1H NMR spectrum for the tantalum-bound ethylene group. Only one signal was observed for the ethylene group in the $^{13}C\{^1H\}$ NMR spectrum, indicating that the C−C vector of the ethylene group must be arranged perpendicular to the mirror plane of symmetry. The $[P_2N_2]$ ligand resonances in the ^1H NMR spectrum are as expected for a complex with apparent C_s symmetry, with four silyl methyl resonances and four ligand methylene proton environments. The resonances associated with the chemically equivalent phenyl substituents of the phosphine ligands are also consistent with this. Variable-temperature ^1H NMR spectroscopy demonstrates that the chemical shift of the β-hydrogens of the ethyl group is significantly temperature dependent, as is one of the resonances of the tantalum bound ethylene group, presumably due to the

(40) Guggenberger, L. G.; Meakin, P.; Tebbe, F. N. *J. Am. Chem. Soc.* **1974**, *96*, 5420.

Scheme 2

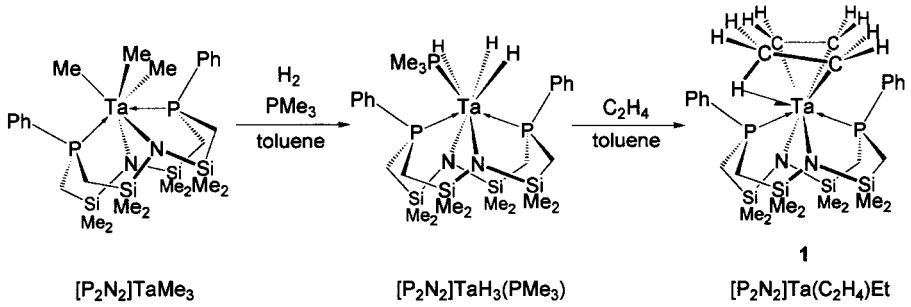

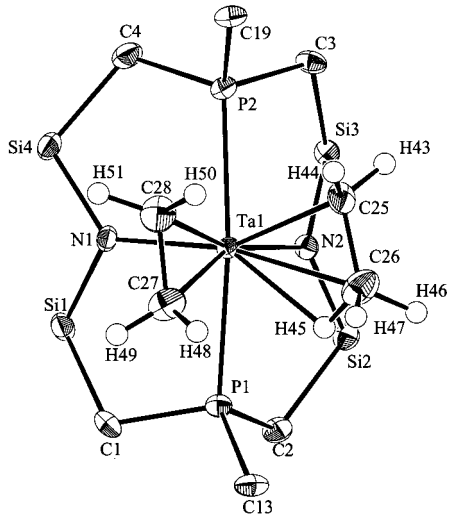

Figure 1. ORTEP diagram of the solid-state molecular structure of $[P_2N_2]Ta(C_2H_4)Et$, **1**, as determined by X-ray crystallography. Silyl methyls have been omitted for clarity and only the ipso carbons of the phenyl rings attached to phosphorus are shown. Selected bond distances (Å), bond angles (deg), and dihedral angels: C(25)−C(26), 1.449(5); C(27)−C(28), 1.449(5); Ta(1)−C(25), 2.251(3); Ta(1)−C(26), 2.498(4); Ta(1)−C(27), 2.251(3); Ta(1)−C(28), 2.362(4); Ta(1)−H(45), 2.07(4); Ta(1)−P(1), 2.5701(8); Ta(1)−P(2), 2.5525(7); Ta(1)−N(1), 2.153(2); Ta(1)−N(2), 2.182(2); C(25)···C(28), 3.038(5); C(26)···C(27), 3.121(5); P(1)−Ta(1)−P(2), 160.18(3); N(1)−Ta(1)−N(2), 97.02(9); P(1)−Ta(1)−N(1)−Si(4), −179.87(14); P(2)−Ta(1)−N(1)−Si(1), 160.93(13); P(1)−Ta(1)−N(2)−Si(3), 163.12(13); P(2)−Ta(1)−N(2)−Si(2), −178.12(14).

Table 1. Crystal Data and Structure Refinement for **1**

compound	**1**[a]
formula	$C_{28}H_{51}N_2P_2Si_4Ta$
fw	770.96
color, habit	orange, irregular
cryst size, mm	0.40 × 0.35 × 0.20
cryst syst	monoclinic
space group	$P2_1/n$ (No. 14)
a, Å	12.0328(8)
b, Å	19.7483(14)
c, Å	14.5850(2)
α, deg	90.
β, deg	92.1381(5)
γ, deg	90.
V, Å^3	3463.4(3)
Z	4
T, °C	−93
ρ_{calc}, g/cm^3	1.478
F(000)	1568.00
radiation	Mo
μ, cm^{-1}	34.20
transmission factors	0.5060−1.000
$2\theta_{max}$, deg	60.1
crystal decay, %	negligible
total no. of reflns	30445
no. of unique reflcns	8914
R_{merge}	0.029
no. with $I \geq n\sigma(I)$	6684
no. of variables	370
R	0.044[a]
R_w	0.043[a]
gof	1.50
max Δ/σ	0.002
residual density e/Å^3	2.09, −1.34 (both near Ta)

[a] Rigaku/ADSC CCD diffractometer, $R = \sum||F_o^2| - |F_c^2||/\sum|F_o^2|$; $R_w = (\sum w(|F_o^2| - |F_c^2|)^2/\sum w|F_o|^4)^{1/2}$.

hydrogens directed toward the ethyl ligand. The ^{1}H NMR signal of the *β*-hydrogens of the ethyl group shifts to lower frequency on cooling. These data indicate that the proposed *β*-agostic interaction in **1** is fluxional, with the entropically disfavored *β*-agostic η^2-ethyl group being increasingly favored at lower temperature. This fluxional process, shown in Figure 2, accounts for the observed C_s symmetry of **1** on the NMR time scale. An in-place rotation of the ethyl group would not account for the apparent C_s symmetry of species **1** in solution.[41]

The intermediate species in Figure 2 is depicted as having an α-agostic interaction, despite the fact that so far no data have been provided as yet to support such an α-agostic−*β*-agostic equilibrium. Evidence for this process in the solution structure of **1** was provided by studying the effect of partial deuteration of the ethyl group.

Isotopic Perturbation of Resonance. It has been noted that between 180 and 350 K the *β*-CH_3 group of the agostic ethyl moiety in **1** shows only a single resonance in the ^{1}H NMR spectrum. Thus, as already mentioned the only evidence for a *β*-agostic interaction in the solution structure of **1** is an unusually low-frequency chemical shift of the *β*-protons and a large coupling of these protons to the phosphorus nuclei of the $[P_2N_2]$ ligand. Evidence for an α-agostic interaction in equilibrium with the *β*-agostic interaction is more difficult to obtain; the chemical shift of the α-protons is anticipated to be affected by the proximity of these protons to the metal center regardless of whether an α-agostic interaction is present, and likewise a three-bond coupling to phosphorus-31 is not unexpected. A valuable technique for examining agostic interactions is isotopic perturbation of resonance (IPR).[42,43] For species with *β*-agostic interactions, this technique involves partially deuterating the *β*-CH_3 group, so that the *β*-CH_2D and *β*-CHD_2 isomers are also present in solution. The difference in the zero-point energies for terminal C−D bonds versus agostic C−D bonds compared to terminal C−H bonds versus agostic C−H bonds causes the protons to accumulate in the *β*-agostic position, whereas the deuterons will accumulate in the terminal sites. Therefore, if

(41) Tempel, D. J.; Brookhart, M. *Organometallics* **1998**, *17*, 2290.

(42) Calvert, R. B.; Shapley, J. R. *J. Am. Chem. Soc.* **1978**, *100*, 7726.

(43) Green, M. L. H.; Hughes, A. K.; Popham, N. A.; Stephens, A. H. H.; Wong, L.-L. *J. Chem. Soc., Dalton Trans.* **1992**, 3077.

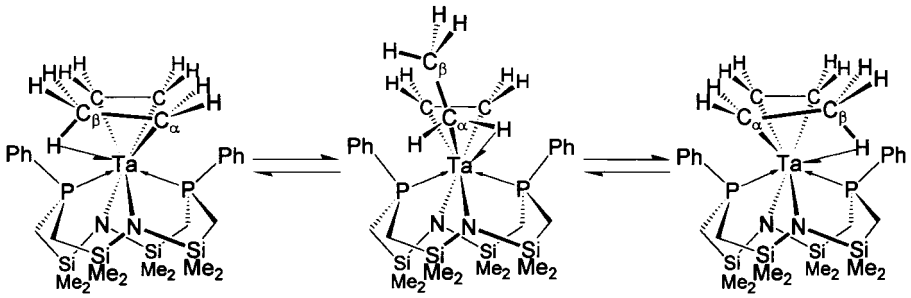

Figure 2. Depiction of the fluxional nature of the β-agostic interaction that results in the C_s symmetry of complex **1** on the NMR time scale. The intermediate species shown here is drawn with an α-agostic interaction.

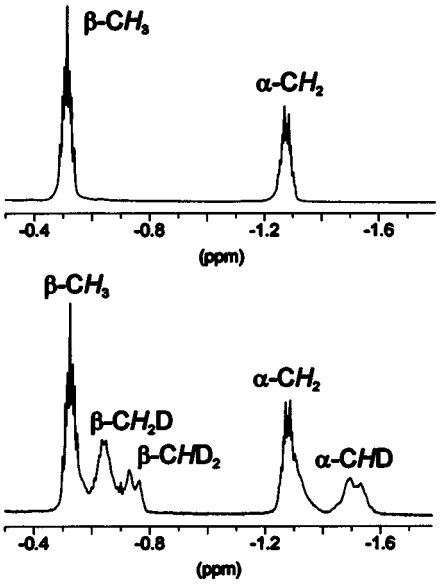

Figure 3. The ethyl region of the ^{1}H NMR (500 MHz, 295 K) spectrum of $[P_2N_2]Ta(C_2H_4)Et$, **1**, before (top) and after (bottom) C_2D_4 was added.

an agostic interaction is present, this experiment should result in an IPR that produces a noticeable chemical shift separation between the isotopomers present.

The preparation of a variety of deuterated isotopomers of **1** proved to be facile. The addition of d_4-ethylene to a solution of **1** provided a mixture of isotopomers. Attempts to monitor this exchange by ^{1}H NMR spectroscopy were unsuccessful, because considerable exchange had already occurred by the time the solution could be transferred to the NMR probe. It is not clear whether the C_2D_4 exchanges with the ethyl group or the bound ethylene or both. Regardless, a mechanism that exchanges proton environments from the ethyl to the ethylene group exists and will be discussed later.

Figure 3 shows the ethyl region of the ^{1}H NMR spectrum of complex **1** before and after a small amount of C_2D_4 has been added. After adding C_2D_4, the resonances for the CH_2CH_3 isotopomer are still the most intense, with the β-CH_3 group at δ −0.52. The β-CH_2D resonance occurs at δ −0.64 ppm, a shift of −0.12 ppm from the undeuterated resonance. The third isotopomer, β-CHD_2, appears at two apparent resonances, with an average chemical shift of δ −0.75; the appearance of two resonances for this signal was unexpected, and it appears to imply that the degree of deuteration of the adjacent methylene group also affects the ^{1}H chemical shift of the β-CHD_2 resonance. The appearance of a large IPR for the α-CH_2 group was also unanticipated. The resonance shifts from δ −1.28 for the α-CH_2 isotopomer to δ −1.52 for the α-CHD isotopomer. The resonance at −1.52 is also comprised of more than one actual chemical shift, so that the $CHDCH_3$ and $CHDCH_2D$ isotopomers, for example, have slightly different ^{1}H chemical shifts for their α-CHD resonances. The effect of deuteration of the bound ethylene moiety has a negligible affect on its apparent chemical shift in the ^{1}H NMR spectrum, as was expected.

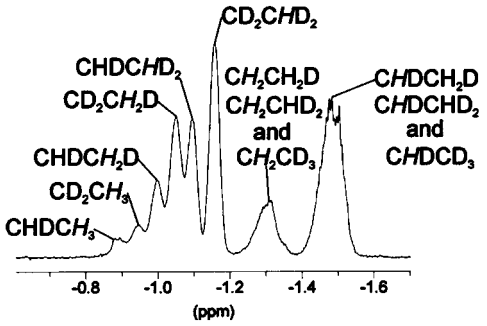

Figure 4. The ethyl region of the ^{1}H NMR (500 MHz, 255 K) spectrum of $[P_2N_2]Ta(C_2H_4)Et$ in which the ethyl group is ∼75% deuterated.

To understand the effect of deuteration of the α-CH_2 group on the chemical shift of the β-CH_3 resonance in the ^{1}H NMR spectrum of **1**, a more highly deuterated sample was prepared which consisted of ∼75% deuterium in the ethyl group. At room temperature, the many signals for the β-C−H group overlap; however, upon cooling the sample to 255 K these signals separate sufficiently to identify at least six distinct resonances. By taking into account the degree of deuteration, it was possible to determine the statistical likelihood of all the possible isotopomers of the ethyl group, and this assisted with assigning the resonances. The ^{1}H spectrum of the ethyl group at 255 K is shown in Figure 4. For the β-CH group, the lowest frequency resonance at δ −1.16 is assigned to the CD_2CHD_2 isotopomer, the resonance at δ −1.10 to the $CHDCHD_2$ isotopomer, and the higher frequency resonances to CD_2CHD_2, $CHDCHD_2$, CD_2CH_3, and $CHDCH_3$, respectively. The resonances of the β-C−H protons in isotopomers containing two protons in the α-C position were too low in intensity to assign. The difference in the chemical shifts of the β-C−H protons compared to the spectrum shown in Figure 3 is due to the temperature dependence of the chemical shifts of these protons, as noted previously. That the lowest frequency corresponds to the most deuterated sites at the β-C is as expected, because this causes the protons to preferentially accumulate in the agostic position.

As mentioned above, the appearance of extra signals in the β-C−H region for isotopomers containing different degrees of deuteration in the α-C position was not expected. The effect of increased deuteration at the α-C position is a decrease in the frequency of the β-C−H resonances. If only the β-agostic interaction was present in the structure of **1** in solution, then only three β-C−H resonances should be observed, and no significant effect should be observed when the α-C is deuterated. However, if an α-agostic interaction is in equilibrium with the

β-agostic interaction, as shown in Figure 2, then the observation of six β-C−H resonances and the large IPR for the α-C−H protons can be rationalized. The origin of this effect is similar to that noted previously, where partial deuteration of the β-C−H group causes the protons to accumulate in the agostic position, due to the slightly higher energy of the deuteron in the agostic position. The effect of increased deuteration of the α-C would provide a slight destabilization of the α-agostic interaction versus the β-agostic interaction. If the energy difference between the β-agostic interaction and the α-agostic interaction is very small, this small destabilization should favor the β-agostic interaction sufficiently to cause the slight shift of the β-C−H resonance to lower frequency, as is observed. The rapid rate of the process shown in Figure 2 is consistent with a small energy difference between the β-agostic and α-agostic ethyl group for **1** in solution.

Unlike the β-C−H resonances, the α-C−H resonances are not greatly affected by the degree of deuteration at the β-C. This is consistent with the observation that the chemical shift of the α-C protons is not greatly temperature dependent, unlike the β-C protons, so that a shift in the equilibrium between the α-agostic and β-agostic structure does not result in a significant change in the chemical shift of the α-C−H resonances. The relatively small temperature dependence of the α-C proton resonance eliminates the possibility that the large IPR observed for **1** is due simply to an equilibrium between a β-agostic and a non-agostic structure. For an IPR to be observed both a difference in chemical shift and a difference in C−H bond length is necessary, and so the significant IPR observed necessitates a structure in which the two α-C−H environments and C−H bond lengths are vastly different in the species lacking a β-agostic interaction. The most probable structure that fits these requirements is one containing an α-agostic interaction, as shown in the center of Figure 2.[44]

The presence of an α-agostic interaction in a tantalum ethyl species such as **1** has precedence; α-agostic interactions are implicated in the formation of tantalum alkylidene complexes from sterically crowded tantalum alkyls,[45] and both α and β hydrogen abstractions have been observed for tantalum alkyls, which presumably proceed through agostic interactions.[46,47] Additionally, examples of niobium ethyl complexes with α-agostic interactions but no evidence of β-agostic interactions have been reported,[30,48] and the zwitterionic tantalocene derivative $(\eta^5\text{-}C_5H_5)_2Ta(=CH_2B(C_6F_5)_3)(Me)$ has a strong α-agostic interaction. To our knowledge, only one example exists where both α-agostic and β-agostic interactions were identified to be in equilibrium in the ^{1}H NMR spectrum;[49] two distinct species corresponding to an α-agostic and a β-agostic niobium bound isopropyl group were observed by ^{1}H NMR spectroscopy, a result that is unique even in that study. For the early transition metals, where both α-agostic and β-agostic interactions are quite common, it is possible that many complexes undergo equilibria of this type; however, such processes may be too fast to be observed on the NMR time scale. In such cases, thorough labeling studies could provide additional information about the solution structures of these complexes. To the best of our knowledge complex **1** provides the first example where an equilibrium between α-agostic and β-agostic interactions is identified by a study of the isotopic perturbation of resonance of both the α and β positions. This could be used to study isolable polymerization catalyst resting states. The absence of other reports of equilibria of this type may be due to the exclusive labeling of the β-C of the ethyl group in other studies,[16,23,24] which prevented the detection of such an equilibrium in solution. On the other hand, for this effect to be observed the α-agostic structure and β-agostic structures must be similar in energy, and this may be uncommon. It has been suggested that the competition between α-agostic and β-agostic interactions is likely largely governed by steric factors, where increasing steric bulk disfavors β-agostic interactions.[30]

NMR Data for Carbon-13 Labeled $[P_2N_2]Ta(^{13}C_2H_4)^{13}Et$. The synthesis of an isotopomer of **1** with the ethyl group carbon-13 labeled was performed to determine the effect of the agostic interactions in species **1** on the $^1J_{CH}$ values. The reaction of $[P_2N_2]Ta{=}CH_2(Me)$ with $^{13}C_2H_4$ yields the species $[P_2N_2]Ta(^{13}C_2H_4)^{13}Et$, where the four carbons of the ethyl and ethylene groups of complex **1** are ^{13}C labeled. The $^{13}C\{^1H\}$ NMR spectrum of this reaction mixture illustrates a $^1J_{CC}$ coupling constant in the ethyl moiety of 30.0 Hz, as is appropriate for a single bond. From the ^{1}H NMR spectrum of this ^{13}C-labeled species, it is possible to determine the $^1J_{CH}$ coupling constants of 126.5 and 123.1 Hz for the α-carbon and β-carbon of the ethyl group, respectively. Both are within the values expected for sp^3 hybridized carbons. In some cases a large $^1J_{CH}$ of ∼150 Hz to the α-carbon has been used as evidence for an agostic interaction;[16,20,24] however, there are other complexes in which β-agostic ethyl groups are implicated where a value similar to that found here was observed.[21] The $^1J_{CH}$ coupling constants for the ethylene fragment are somewhat obscured in the ^{1}H NMR spectrum, as these signals are in the same region as the ligand methylene groups. From the ^{13}C NMR data these coupling constants were ∼145 Hz. These are larger than those observed for the ethyl group, but smaller than the ∼156 Hz coupling constant expected for ethylene complexes with minimal back-bonding.

The variable-temperature ^{13}C NMR spectrum of $[P_2N_2]Ta(^{13}C_2H_4)^{13}Et$ was also investigated to complement the variable-temperature ^{1}H NMR data obtained for **1**. The resonance of the α-C shifts from δ 75.9 at 350 K to δ 53.5 at 180 K, and the corresponding $^1J_{CH}$ value increases from 123.4 Hz at 350 K to 133.6 Hz at 233 K. These data are consistent with an increased contribution from an α-agostic structure versus a β-agostic structure at higher temperatures.[15,20] The resonance of the β-C is less strongly affected and shifts from δ 7.3 at 350 K to δ 2.0 at 180 K and the corresponding $^1J_{CH}$ value changes from 123.8 Hz at 350 K to 122.8 Hz at 233 K. In comparison, the resonance of the tantalum bound ethylene group is δ 45.5 at 350 K and δ 43.3 at 180 K, which indicates that this resonance is not greatly affected by temperature.

NMR Data for $[P_2N_2]Ta(C_2H_4)Me$ (2). The ethylene methyl complex, **2**, is produced as a minor product in the reaction of $[P_2N_2]Ta{=}CH_2(Me)$ with ethylene. The ^{1}H NMR spectrum of complex **2** contains a low-frequency resonance for the tantalum-bound methyl group at δ −1.49 coupled to phosphorus ($^3J_{PH}$ = 3.1 Hz). In complex **2** four silyl methyl peaks are present in

(44) A fast equilibrium between an ethylene ethyl and an ethyl ethylidene structure, formed from an α-hydrogen abstraction from the ethyl group and insertion of this hydride into the ethylene moiety, is not a viable mechanism. Such a process would rapidly exchange the chemical environment at the α-position of the ethyl group in the ethylene ethyl structure with the chemical environments of the ethylene moiety, and this is not observed in the ^{1}H NMR spectrum. An EXSY spectrum (vide infra) further demonstrates that this process does not occur even on a time scale too slow to be observed in the ^{1}H NMR spectrum.

(45) Schrock, R. R. *Acc. Chem. Res.* **1979**, *12*, 98.
(46) Freundlich, J. S.; Schrock, R. R.; Davis, W. M. *J. Am. Chem. Soc.* **1996**, *118*, 3643.
(47) Freundlich, J. S.; Schrock, R. R.; Davis, W. M. *Organometallics* **1996**, *15*, 2777.
(48) Hierso, J. C.; Etienne, M. *Eur. J. Inorg. Chem.* **2000**, *5*, 839.
(49) Jaffart, J.; Mathieu, R.; Etienne, M.; McGrady, J. E.; Eisenstein, O.; Maseras, F. *Chem. Commun.* **1998**, 2011.

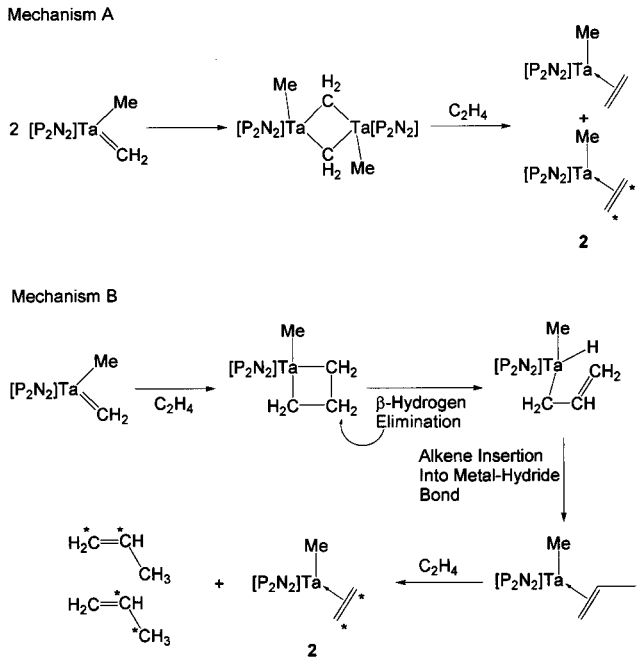

Figure 5. Two possible mechanisms for the formation of $[P_2N_2]Ta(C_2H_4)Me$, **2**. The starred carbon atoms illustrate where carbon-13 labels would appear in the products if the reaction was performed with $^{13}C_2H_4$.

the ^{1}H NMR spectrum, indicating that, as for species **1**, this complex appears to have C_s symmetry. Unfortunately, other peaks in the same region, particularly the $[P_2N_2]$ ligand methylene signals, obscure the ^{1}H NMR signals for the ethylene protons. An α-agostic interaction may be present in this species; however, we have not probed this possibility by IPR.

For complex **2**, a single isotopomer $[P_2N_2]Ta(^{13}C_2H_4)Me$ results from the reaction of $[P_2N_2]Ta{=}CH_2(Me)$ with $^{13}C_2H_4$. The $^{13}C\{^1H\}$ NMR spectrum contains a signal for the tantalum-bound ethylene group at δ 49.1, near that observed for the ethylene group in complex **1**. The tantalum methyl group of **2** is not ^{13}C labeled, and appears as a triplet at δ 51.4.

Mechanism of the Reaction of Ethylene with $[P_2N_2]Ta{=}CH_2(Me)$. Previous studies on the thermal decomposition of the 18-electron complex $(\eta^5\text{-}C_5H_5)_2Ta{=}CH_2(Me)$ demonstrated that it decomposed via dimerization and coupling of the two bridging methylidene moieties.[32,50] The species $(\eta^5\text{-}C_5H_5)_2Ta(C_2H_4)Me$ resulted, where the ethylene unit is derived from the coupled methylidene units. The remaining "$(\eta^5\text{-}C_5H_5)_2TaMe$" moiety could be trapped using ethylene. This same mechanism could be responsible for the formation of methyl complex **2**, and is illustrated in Figure 5 as mechanism A. The starred carbon atoms indicate where the ^{13}C labels would be expected if the reaction was performed with $^{13}C_2H_4$.

An alternative mechanism to the formation of complex **2** would involve initial metallocyclobutane formation upon addition of ethylene to the tantalum methylidene, and subsequent decomposition of this intermediate by β-hydrogen elimination. Reinsertion of the resulting olefin into the hydride bond in the opposite manner would generate a propylene complex, $[P_2N_2]Ta(CH_2{=}CHMe)Me$, which could then further react with ethylene, eliminating propylene and generating complex **2**, as shown in Figure 5 as mechanism B. As for mechanism A, the starred carbon atoms indicate where the ^{13}C labels would be expected in the products if the reaction was performed with $^{13}C_2H_4$.

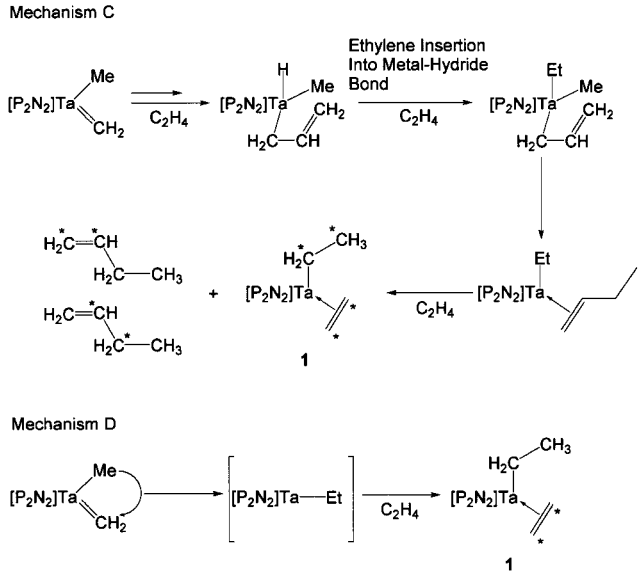

Figure 6. Two possible reaction mechanisms for the formation of $[P_2N_2]Ta(C_2H_4)Et$, **1**, from the reaction of ethylene with $[P_2N_2]Ta{=}CH_2(Me)$. The starred carbon atoms illustrate where carbon-13 labels would appear in the products if the reaction was performed with $^{13}C_2H_4$.

Inspection of the $^{13}C\{^1H\}$ NMR spectrum of the products of the reaction of $[P_2N_2]Ta{=}CH_2(Me)$ with $^{13}C_2H_4$ reveals that indeed two isotopomers of propylene are produced, $^{13}CH_2{=}^{13}CHCH_3$ and $H_2C{=}^{13}CH^{13}CH_3$, clearly supportive of mechanism B. The tantalum-bound ethylene moiety is fully labeled, and the tantalum methyl group remains unlabeled. The metallocyclobutane product once formed appears to decompose rapidly, as it does not accumulate in solution, and no productive metathesis, to form $[P_2N_2]Ta{=}^{13}CH_2(Me)$ and $^{13}CH_2{=}CH_2$, is observed.

The mechanism of formation of the ethyl complex **2** could involve a similar mechanism to that proposed for complex **1**. Initial metallocyclobutane formation could be followed by β-hydrogen elimination; however, if instead of reinserting into the double bond to form a propylene complex ethylene inserts into the hydride bond, $[P_2N_2]Ta(CH_2CH{=}CH_2)MeEt$ would form. If insertion of the double bond into the tantalum methyl bond then occurs a butene complex would be formed, which could exchange with ethylene to form the ethyl complex **1** and 1 equiv of butene. This mechanism is labeled mechanism C in Figure 6.

A second, simpler mechanism is also shown in Figure 6, mechanism D. In this case the methylidene inserts into the tantalum−methyl bond, forming an ethyl complex, which is then trapped by ethylene. The migratory insertion of an alkylidene into a cis tantalum alkyl linkage has been demonstrated to occur with cationic tungsten complexes,[51−53] late transition metal carbene complexes,[54,55] and a niobium alkylidene bearing electron-withdrawing substituents,[56] presumably because these factors render the alkylidene more electrophilic. However, evidence suggests that this insertion is not restricted to electrophilic alkylidenes, as the insertion of an alkylidene into a tantalum alkyl has been proposed as a reaction step in the

(50) Schrock, R. R.; Sharp, P. R. *J. Am. Chem. Soc.* **1978**, *100*, 2389.
(51) Hayes, J. C.; Pearson, J. D. N.; Cooper, N. J. *J. Am. Chem. Soc.* **1981**, *106*, 3026.
(52) Hayes, J. C.; Cooper, N. J. *J. Am. Chem. Soc.* **1982**, *104*, 5570.
(53) Jernakoff, P.; Cooper, N. J. *J. Am. Chem. Soc.* **1984**, *106*, 3026.
(54) Thorn, D. L.; Tulip, T. H. *J. Am. Chem. Soc.* **1981**, *103*, 5984.
(55) Kleitzein, H.; Werner, H.; Serhadli, P.; Ziegler, M. L. *Angew. Chem., Int. Ed. Engl.* **1983**, *22*, 46.
(56) Threlkel, R. S.; Bercaw, J. E. *J. Am. Chem. Soc.* **1981**, *103*, 2650.

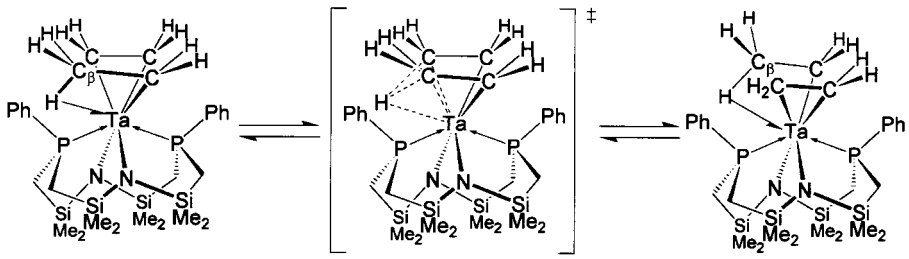

Figure 7. Depiction of the mechanism believed to exchange the proton environments of the ethyl and ethylene ligands of species **1**.

decomposition of alkylidenes only slightly more sterically crowded than $(\eta^5\text{-}C_5H_5)_2Ta{=}CH_2(Me)$, such as the ethylidene complex $(\eta^5\text{-}C_5H_5)_2Ta{=}CH_2Me(Me)$.[57]

A labeling study here should reveal if mechanism C or mechanism D occurs in the formation of ethyl complex **1**. In Figure 6, the starred carbon atoms indicate where the labeled atoms are anticipated to be if the reaction of $[P_2N_2]Ta{=}CH_2(Me)$ is performed with $^{13}C_2H_4$. Although ^1H, $^{13}C\{^1H\}$, and $^{31}P\{^1H\}$ NMR spectroscopies identify the tantalum product as the completely labeled species $[P_2N_2]Ta(^{13}C_2H_4)^{13}CH_2{}^{13}CH_3$, as is predicted for mechanism C, the 1-butene observed in the product mixture is fully labeled $^{13}CH_2{=}{}^{13}CH^{13}CH_2{}^{13}CH_3$, rather than the partially labeled 1-butene that is anticipated from mechanism C. The 1-butene observed is therefore simply produced from the dimerization of ethylene. The similar amount of 1-butene and **1** produced in the reaction of $[P_2N_2]TaMe_3$ with ethylene therefore must be coincidental. Examples of tantalum complexes that catalyze the dimerization ethylene and also produce higher oligomers are known; however, neither complex **1** nor **2** catalyzes these reactions, so intermediates or trace impurities must be involved in 1-butene production. Mechanism D is therefore most consistent with the data in the formation of **1**. The formation of the fully labeled product can be rationalized by the exchange of the bound ethyl group with the carbon-13 labeled ethylene. This exchange has been noted before in the reaction of C_2D_4 with $[P_2N_2]Ta(C_2H_4)Et$ to produce partially deuterated isotopomers. The reaction of $[P_2N_2]Ta{=}CH_2(Me)$ with C_2D_4 in a sealed NMR tube results in the appearance of a resonance in the ^1H NMR spectrum in the region anticipated for ethylene. This resonance is slightly broadened, presumably because isotopomers such as C_2D_3H are the end products. This provides further evidence that despite forming the fully labeled product, mechanism D is the likely mechanism for the formation of **1**.

The ability of complex **1** to react with labeled ethylene such as $^{13}C_2H_4$ to exchange both the ethylene and ethyl groups can be explained by two possible mechanisms. The most obvious mechanism would involve β-elimination of ethylene to form an ethylene hydride, $[P_2N_2]Ta(C_2H_4)H$, which could then react with $^{13}C_2H_4$ to generate the labeled product. The stability of **1** in air and the observation that ethylene is not lost from solutions of **1** over several days indicates that the mechanism is probably not this straightforward. The bound ethylene moiety could also be involved in an exchange mechanism by which the insertion of ethylene into the bound ethylene forms a metallocyclopentane, which can then eliminate ethylene and result in exchange. This olefin exchange mechanism is believed to occur in the mechanism of the formation of **2**, where propylene is displaced by ethylene, and therefore seems a likely mechanism for the exchange of free ethylene with bound ethylene in **1**.

Exchange of Proton Environments in Ethyl Complex 1. The rapid rate at which deuterium is scrambled into both the tantalum−ethyl and tantalum−ethylene groups when **1** is reacted with C_2D_4 strongly suggests the existence of a fluxional process that interconverts the tantalum ethyl and tantalum ethylene groups. Such a process is known to occur in the cationic late transition metal complex $[(\eta^5\text{-}C_5H_5)Co(\eta^2\text{-}C_2H_4)(\eta^2\text{-}Et)]^+$, where the intermediate is the bis(ethylene) hydride $[(\eta^5\text{-}C_5Me_5)Co(\eta^2\text{-}C_2H_4)_2H]^+$.[58,59] Despite this precedent, this mechanism seems unlikely in complex **1**. Although the metal center in species **1** could formally be considered Ta(III), with a d^2 configuration, extensive back-bonding to the tantalum ethylene moiety suggests the complex is more accurately described as a Ta(V) metallacyclopropane, with no remaining metal-based electrons, and no available higher oxidation states. Because it lacks the electrons necessary to allow back-bonding to two ethylene moieties to form $[P_2N_2]Ta(C_2H_4)_2H$, complex **1** would be more likely to eliminate ethylene to form $[P_2N_2]Ta(C_2H_4)H$. Although solutions of **1** turn green over the course of several months in the absence of ethylene due to a trace amount of a new complex, the species $[P_2N_2]Ta(C_2H_4)H$ could not be detected by ^1H NMR, and the slow rate at which this decomposition reaction occurs prohibits it from being of importance in the more rapid exchange of proton environments described here. Interestingly, many ethylene ethyl compounds have been prepared, and to our knowledge (with the exception of the previously mentioned cobalt example) none exhibits β-agostic interactions or fluxional processes that exchange ethyl and ethylene proton environments.[60−63]

Examining the crystal structure of **1**, it is notable that the bond lengths in the tantalum ethyl ligand and the tantalum ethylene ligand are remarkably similar. The C−C bond lengths are identical, and the $Ta{-}C_\alpha$ distance is identical to one of the Ta−C bond lengths of the bound ethylene. The $Ta{-}C_\beta$ interaction is only 0.136 Å longer than the longer Ta−C bond lengths in to the bound ethylene. Considering the structural similarities between the ethylene and ethyl ligands in species **1**, a valid mechanism for the exchange of proton environments in complex **1** could simply involve direct transfer of a hydrogen atom from the ethyl group to the ethylene group, as shown in Figure 7. The β-agostic interaction will weaken the C−H bond that is interacting with the metal center in the ground state, and in the postulated intermediate the hydrogen atom that is

(57) Sharp, P. R.; Schrock, R. R. *J. Organomet. Chem.* **1979**, *171*, 43.
(58) Brookhart, M.; Lincoln, D. M.; Bennett, M. A.; Pelling, S. *J. Am. Chem. Soc.* **1990**, *112*, 2691.
(59) Brookhart, M.; Green, M. L. H.; Pardy, R. B. A. *J. Chem. Soc., Chem. Commun.* **1983**, 691.
(60) Basickes, N.; Hutson, A. C.; Sen, A.; Yap, G. P. A.; Rheingold, A. L. *Organometallics* **1996**, *15*, 4116.
(61) Spencer, M. D.; Morse, P. M.; Wilson, S. R.; Girolami, G. S. *J. Am. Chem. Soc.* **1993**, *115*, 2057.
(62) Férnandez, F. J.; Gómez-Sal, P.; Manzanero, A.; Royo, P.; Jacobsen, H.; Berke, H. *Organometallics* **1997**, *16*, 1553.
(63) Barry, J. T.; Chacon, S. T.; Chisholm, M. H.; Huffman, J. C.; Streib, W. E. *J. Am. Chem. Soc.* **1995**, *117*, 1974.

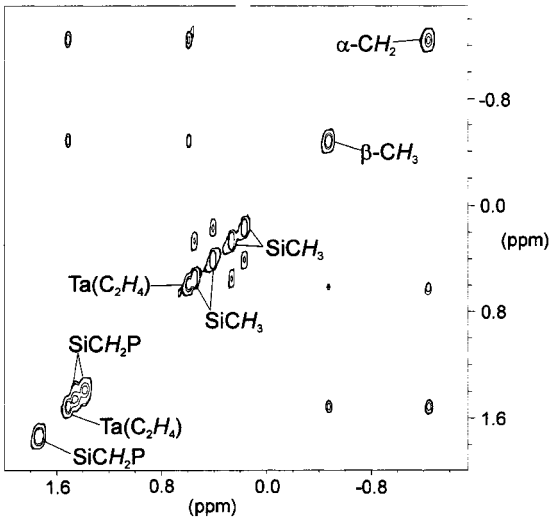

Figure 8. A portion of the EXSY spectrum ($\tau = 0.4$ s) of $[P_2N_2]Ta(C_2H_4)Et$, illustrating four cross-signals between the ethyl and ethylene ligands, and cross-signals between pairs of silyl−methyl environments.

transferred has bonding interactions with two carbon atoms and the tantalum center.

Unfortunately, the rate at which this exchange reaction occurs is too slow to be monitored by variable-temperature ^{1}H NMR. In an attempt to verify that this process does occur even in the absence of a labeled ethylene such as C_2D_4, a phase-sensitive EXSY (exchange spectroscopy)[64,65] spectrum of complex **1** was obtained at 300 K, and a portion of this spectrum is shown in Figure 8. This 2-D spectrum displays four cross-signals of the correct sign and intensity to be due to chemical exchange between both resonances of the ethyl unit and both resonances of the tantalum ethylene, thus indicating that as implied from the mechanism shown in Figure 7, exchange between both ethyl group environments and both ethylene ligand environments is possible. Another possible mechanism,[20] involving transfer of an α-agostic hydrogen atom from the ethyl group to generate the intermediate $[P_2N_2]Ta{=}CHMe(Et)$, would not allow for exchange of all the observed chemical environments. Furthermore, cross-signals occur between pairs of the ligand silyl methyl environments, as would be expected if a fluxional process occurred which exchanged the location of the ethyl and ethylene ligands in complex **1**. Cross-signals between pairs of ligand methylene environments should also be observed; however, it appears that the pairs of signals are too close together (δ 1.34, 1.41; 1.70, 1.70) for these cross-signals to be distinguishable from the large diagonal signals.

Conclusions

The reaction of $[P_2N_2]Ta{=}CH_2(Me)$ with ethylene produces the complex $[P_2N_2]Ta(C_2H_4)Et$ (**1**) as the main product along with $[P_2N_2]Ta(C_2H_4)Me$ (**2**). Extensive evidence exists for a β-agostic interaction in **1**, and this same interaction was also present in the solid-state X-ray structure. By careful examination of the ^{1}H NMR spectrum of a mixture of partially deuterated isotopomers of **1**, evidence was collected that supports an equilibrium between the β-agostic structure and an α-agostic interaction of the ethyl ligand in solution. Such interactions are of great importance in early transition metal olefin polymerization catalysts, and this complex is particularly interesting because it contains an ethyl ligand arranged cis to an ethylene ligand. However, no polymerization activity is noted in this complex due to this considerable back-bonding to the ethylene ligand. The elongation of the C−C bond of the ethylene unit from this back-bonding interaction renders the geometry of the bound ethylene quite similar to that of the β-agostic ethyl ligand. This similarity in structure undoubtedly assists in an exchange process whereby the β-agostic hydrogen atom from the ethyl group is transferred to the ethylene moiety, exchanging these groups without the intermediacy of an ethylene hydride species, a process that is believed to be important in olefin polymerization chain termination.[66]

Experimental Section

Unless otherwise stated all manipulations were performed under an atmosphere of dry oxygen-free dinitrogen by means of standard Schlenk or glovebox techniques (Vacuum Atmospheres HE-553-2 glovebox equipped with a MO-40-2H purification system and a −40 °C freezer). Hexanes were predried by refluxing over CaH_2, and then distilled under argon from sodium benzophenone ketyl with tetraglyme added to solubilize the ketyl. Anhydrous diethyl ether was stored over sieves and distilled from sodium benzophenone ketyl under argon. Toluene was predried by refluxing over CaH_2 and then distilled from sodium under argon. Nitrogen was dried and deoxygenated by passing the gases through a column containing molecular sieves and MnO. Deuterated benzene and toluene were dried by refluxing with molten potassium metal, and molten sodium metal, respectively, in a sealed vessel under reduced pressure, then trap-to-trap distilled, and freeze−pump−thaw degassed three times. Unless otherwise stated, ^{1}H, ^{31}P, ^{1}H{^{31}P}, ^{13}C{^{1}H}, ^{13}C, and variable-temperature NMR spectra were recorded on a Bruker AMX-500 Instrument operating at 500.1 MHz for ^{1}H spectra. ^{1}H NMR spectra were referenced to internal C_6D_5H (7.15 ppm), $CDHCl_2$ (5.32 ppm), and C_7D_7H (2.09 ppm), ^{31}P{^{1}H} NMR spectra to external $P(OMe)_3$ (141.0 ppm with respect to 85% H_3PO_4 at 0.0 ppm), and ^{13}C spectra to $^{13}CC_5D_6$ (128.4 ppm) and $^{13}CD_2Cl_2$ (54.0 ppm). Elemental analyses were performed by Mr. P. Borda of this department.

Photolysis of $[P_2N_2]TaMe_3$ under C_2H_4. A sample of $[P_2N_2]TaMe_3$ (1.05 g, 1.38 mmol) in 100 mL of hexanes was sealed in a glass vessel equipped with a Teflon valve under an atmosphere of ethylene. The vessel was exposed to a Vitalux sunlamp for 30 min and then stirred for two weeks at room temperature. The ethylene was then removed under vacuum, and an orange solid (0.55 g) crystallized that had poor solubility in hexanes but was soluble in aromatic solvents. The solid was identified as a mixture of $[P_2N_2]Ta(C_2H_4)Et$ (**1**) and $[P_2N_2]Ta(C_2H_4)Me$ (**2**). Exact ratios and yields of these products depended considerably on the conditions used, such as photolysis duration and intensity, but $[P_2N_2]Ta(C_2H_4)Et$ was always the major product. A product ratio of compounds **1** to **2** as high as 10:1 and as low as 2:1 was observed. Both compounds **1** and **2** are air stable but moisture sensitive. ^{1}H NMR of selected peaks (C_6D_6, 295 K, 500 MHz): δ −1.49 (t, $^3J_{PH} = 3.1$ Hz, $[P_2N_2]Ta(C_2H_4)CH_3$), −1.28 ($A_2M_3X_2$, $^3J_{HH} = 7.8$ Hz, $^3J_{HP} = 3.1$ Hz, $[P_2N_2]Ta(C_2H_4)CH_2CH_3$), −0.53 ($A_3M_2X_2$, $^3J_{HH} = 7.8$ Hz, $J_{HP} = 4.4$ Hz, $[P_2N_2]Ta(C_2H_4)CH_2CH_3$), 0.13, 0.23, 0.37, and 0.51 (s, $[P_2N_2]Ta(C_2H_4)Et$ ligand $SiCH_3$), −0.01, 0.30, 0.46, and 0.58 (s, $[P_2N_2]Ta(C_2H_4)Me$ ligand $SiCH_3$).

Photolysis of $[P_2N_2]TaMe_3$ under $^{13}C_2H_4$. A sample of $[P_2N_2]TaMe_3$ (20 mg, 0.026 mmol) in 1 mL of C_6D_6 was sealed in a NMR tube under 1 atm of $^{13}C_2H_4$. The tube was exposed to a Vitalux sunlamp for 30 min and then stirred for two weeks at room temperature. The two NMR-active tantalum-containing products were identified as $[P_2N_2]Ta(^{13}C_2H_4)^{13}Et$ and $[P_2N_2]Ta(^{13}C_2H_4)Me$ and were present in approximately a 2:1 ratio. The ^{13}C NMR spectrum identified the 1-butene isotopomer as the fully ^{13}C-labeled $^{13}CH_2{=}^{13}CH_2{}^{13}CH_2{}^{13}CH_3$ and the two propylene isotopomers as $CH_2{=}^{13}CH_2{}^{13}CH_3$ and $^{13}CH_2{=}^{13}CH_2{-}CH_3$. ^{1}H NMR, selected peaks (C_6D_6, 299 K, 500 MHz): δ −1.51 (t, $[P_2N_2]Ta(^{13}C_2H_4)CH_3$), −1.29 (m, $^1J_{CH} = 126.8$ Hz, $[P_2N_2]Ta^{13}CH_2{-}{}^{13}CH_3$), −0.52 (m, $^1J_{CH} = 123.2$ Hz, $[P_2N_2]TaCH_2CH_3$). ^{31}P(C_6D_6, 299 K): δ 21.3 (vt, $^2J_{CP} = 4.2$ Hz, $[P_2N_2]Ta(^{13}C_2H_4)Me$), 24.0 (m, $[P_2N_2]Ta(^{13}C_2H_4)^{13}Et$). ^{13}C{^{1}H} NMR ($C_6D_6$, 299 K, 129.76 MHz): δ 6.3

(64) Jeener, J.; Meier, B. H.; Bachmann, P.; Ernst, R. R. *J. Chem. Phys.* **1979**, *71*, 4546.
(65) Perrin, C. L.; Dwyer, T. J. *Chem. Rev.* **1990**, *90*, 935.
(66) Margl, P.; Deng, L.; Ziegler, T. *J. Am. Chem. Soc.* **1999**, *121*, 154.

(dt, $^1J_{CC}$ = 30.0 Hz, $^2J_{PC}$ = 4.5 Hz, [P₂N₂]Ta($^{13}C_2H_4$)$^{13}CH_2{}^{13}C$H₃), 13.6 (ddd, $^1J_{CC}$ = 34.5 Hz, $^2J_{CC}$ = 2.2, $^3J_{CC}$ = 4.2, $^{13}CH_2$=$^{13}CH_2{}^{13}CH_2{}^{13}C$H₃), 19.7 (d, $^2J_{CC}$ = 42.2 Hz, CH₂=$^{13}CH_2{}^{13}C$H₃), 27.3 (dd, $^1J_{CC}$ = 34.3 Hz, $^1J_{CC}$ = 41.5 Hz, $^{13}CH_2$=$^{13}CH_2{}^{13}CH_2{}^{13}CH_3$), 45.1 (vt, $^2J_{PC}$ = 4.8 Hz, [P₂N₂]Ta($^{13}C_2H_4$)^{13}Et), 49.1 (vt, $^2J_{PC}$ = 4.2 Hz, [P₂N₂]Ta($^{13}C_2H_4$)Me), 70.6 (dt, $^1J_{CC}$ = 30.0 Hz, $^2J_{PC}$ = 9.0 Hz, [P₂N₂]Ta($^{13}C_2H_4$)$^{13}CH_2{}^{13}CH_3$), 113.8 (dd, $^1J_{CC}$ = 69.9 Hz, $^3J_{CC}$ = 4.2 Hz, $^{13}CH_2$=$^{13}CH_2{}^{13}CH_2{}^{13}CH_3$), 116.2 (d, $^1J_{CC}$ = 69.5 Hz, $^{13}CH_2$=$^{13}CH_2CH_3$), 134.0 (d, $^1J_{CC}$ = 69.9 Hz, $^{13}CH_2$=$^{13}CH_2CH_3$), 134.0 (d, $^1J_{CC}$ = 42.2 Hz, CH₂=$^{13}CH_2{}^{13}CH_3$), 140.8 (ddd, $^1J_{CC}$ = 69.9 Hz, $^1J_{CC}$ = 41.5 Hz, $^2J_{CC}$ = 2.2 Hz, $^{13}CH_2$=$^{13}CH_2{}^{13}CH_2{}^{13}CH_3$). ^{13}C NMR (C₆D₆, 299 K, 129.76 MHz): δ 6.3 (dt, $^1J_{CC}$ = 30.0 Hz, $^1J_{CH}$ = 123.2 Hz, [P₂N₂]Ta($^{13}C_2H_4$)$^{13}CH_2{}^{13}CH_3$), 45.1 (m, $^1J_{CH}$ ~ 140 Hz, [P₂N₂]Ta($^{13}C_2H_4$)^{13}Et), 49.1 (m, $^1J_{CH}$ ~ 140 Hz, [P₂N₂]Ta($^{13}C_2H_4$)Me), 70.6 (dt, $^1J_{CC}$ = 30.0 Hz, $^1J_{CH}$ = 126.8 Hz, [P₂N₂]-Ta($^{13}C_2H_4$)$^{13}CH_2{}^{13}CH_3$).

Variable-Temperature ^{13}C NMR spectra of [P₂N₂]Ta($^{13}C_2H_4$)^{13}Et. ^{13}C NMR, selected peaks (C₇D₈, 350 K, 129.76 MHz): δ 7.3 (m, $^1J_{CH}$ = 123.8 Hz, [P₂N₂]Ta($^{13}C_2H_4$)$^{13}CH_2{}^{13}CH_3$), 45.5 (m, [P₂N₂]Ta($^{13}C_2H_4$)^{13}Et), 75.9 (m, $^1J_{CH}$ = 123.4 Hz, [P₂N₂]Ta($^{13}C_2H_4$)$^{13}CH_2{}^{13}CH_3$). ^{13}C NMR, selected peaks (C₇D₈, 330 K, 129.76 MHz): δ 6.7 (m, $^1J_{CH}$ = 123.6 Hz, [P₂N₂]Ta($^{13}C_2H_4$)$^{13}CH_2{}^{13}CH_3$), 45.2 (m, [P₂N₂]Ta($^{13}C_2H_4$)^{13}Et), 73.4 (m, $^1J_{CH}$ = 125.3 Hz, [P₂N₂]Ta($^{13}C_2H_4$)$^{13}CH_2{}^{13}CH_3$). ^{13}C NMR, selected peaks (C₇D₈, 300 K, 129.76 MHz): δ 5.7 (m, $^1J_{CH}$ = 123.7 Hz, [P₂N₂]-Ta($^{13}C_2H_4$)$^{13}CH_2{}^{13}CH_3$), 44.7 (m, [P₂N₂]Ta($^{13}C_2H_4$)^{13}Et), 69.3 (m, $^1J_{CH}$ = 127.5 Hz, [P₂N₂]Ta($^{13}C_2H_4$)$^{13}CH_2{}^{13}CH_3$). ^{13}C NMR, selected peaks (C₇D₈, 273 K, 129.76 MHz): δ 4.8 (m, $^1J_{CH}$ = 123.1 Hz, [P₂N₂]Ta-($^{13}C_2H_4$)$^{13}CH_2{}^{13}CH_3$), 44.2 (m, [P₂N₂]Ta($^{13}C_2H_4$)^{13}Et), 65.4 (m, $^1J_{CH}$ = 128.5 Hz, [P₂N₂]Ta($^{13}C_2H_4$)$^{13}CH_2{}^{13}CH_3$). ^{13}C NMR, selected peaks (C₇D₈, 253 K, 129.76 MHz): δ 4.1 (m, $^1J_{CH}$ = 123.1 Hz, [P₂N₂]Ta-($^{13}C_2H_4$)$^{13}CH_2{}^{13}CH_3$), 44.0 (m, [P₂N₂]Ta($^{13}C_2H_4$)^{13}Et, 62.6 (m, $^1J_{CH}$ = 131.1 Hz, [P₂N₂]Ta($^{13}C_2H_4$)$^{13}CH_2{}^{13}CH_3$). ^{13}C NMR, selected peaks (C₇D₈, 233 K, 129.76 MHz): δ 3.5 (m, $^1J_{CH}$ = 122.8 Hz, [P₂N₂]Ta-($^{13}C_2H_4$)$^{13}CH_2{}^{13}CH_3$), 43.7 (m, [P₂N₂]Ta($^{13}C_2H_4$)^{13}Et), 59.9 (m, $^1J_{CH}$ = 133.6 Hz, [P₂N₂]Ta($^{13}C_2H_4$)$^{13}CH_2{}^{13}CH_3$). ^{13}C NMR, selected peaks (C₇D₈, 213 K, 129.76 MHz): δ 2.8 (m, [P₂N₂]Ta($^{13}C_2H_4$)$^{13}CH_2{}^{13}CH_3$), 43.5 (m, [P₂N₂]Ta($^{13}C_2H_4$)^{13}Et), 57.2 (m, [P₂N₂]Ta($^{13}C_2H_4$)$^{13}CH_2{}^{13}CH_3$). ^{13}C NMR, selected peaks (C₇D₈, 193 K, 129.76 MHz): δ 2.3 (m, [P₂N₂]-Ta($^{13}C_2H_4$)$^{13}CH_2{}^{13}CH_3$), 43.3 (m, [P₂N₂]Ta($^{13}C_2H_4$)^{13}Et), 55.0 (m, [P₂N₂]-Ta($^{13}C_2H_4$)$^{13}CH_2{}^{13}CH_3$). ^{13}C NMR, selected peaks (C₇D₈, 180 K, 129.76 MHz): δ 2.0 (m, [P₂N₂]Ta($^{13}C_2H_4$)$^{13}CH_2{}^{13}CH_3$), 43.2 (m, [P₂N₂]Ta-($^{13}C_2H_4$)^{13}Et), 53.5 (m, [P₂N₂]Ta($^{13}C_2H_4$)$^{13}CH_2{}^{13}CH_3$).

Photolysis of [P₂N₂]TaMe₃ under C₂D₄. A sample of [P₂N₂]TaMe₃ (20 mg, 0.026 mmol) in 1 mL of C₆D₆ was sealed in a NMR tube under 1 atm of C₂D₄. The tube was exposed to a Vitalux sunlamp for 30 min and then stirred for two weeks at room temperature.

Synthesis of [P₂N₂]TaH₃(PMe₃) (3). A yellow solution of [P₂N₂]-TaMe₃ (1.00 g, 1.32 mmol) in 120 mL of ether was transferred to a 500 mL thick wall glass vessel equipped with a Teflon valve and stir bar. The mixture was degassed, and a 5-fold excess of PMe₃ was vacuum transferred into the reaction vessel, which was then sealed under 4 atm of hydrogen gas. The mixture was stirred for 3 days in the absence of light. The solution was then evaporated to dryness and the resulting solid was rinsed with minimal pentanes, filtered, and dried, yielding red [P₂N₂]TaH₃(PMe₃) in 95% yield. Some ^{1}H NMR coupling constants were determined with the assistance of Lorentz−Gaussian resolution enhancement. ^{1}H NMR (500 MHz, C₆D₆, 30 °C): δ 0.34, 0.38, 0.38, 0.39, 0.40, 0.40, 0.53, and 0.65 (s, 24H total, SiC*H*₃), 0.67 (d, $^2J_{HP}$ = 7.2 Hz, 9H, P(C*H*₃)₃), 0.87 and 1.27 (AMX, $^2J_{HH}$ = 13.9 Hz, 2H total, C*H*₂ ring), 1.40 (ABX, $^2J_{HH}$ = 14.3 Hz, 1H, C*H*₂ ring), 1.44 (ABMX, $^2J_{HH}$ = 14.3 Hz, $^4J_{HH}$ = 1.4 Hz, 1H, C*H*₂ ring), 1.54 and 2.10 (AMX, $^2J_{HH}$ = 14.4 Hz, 2H total, C*H*₂ ring), 1.56 and 1.73 (AMX, $^2J_{HH}$ = 13.4 Hz, 2H total, C*H*₂ ring), 7.08 and 7.10 (m, 2H total, PPh *p-H*), 7.17 and 7.22 (m, 4H total, PPh *m-H*), 7.80 (AMNXYZ, J_{HP} = 110 Hz, J_{HP} = 104 Hz, $J_{HP(B)}$ = 18.6 Hz, $^2J_{HH(B)}$ = 7.1 Hz, $^2J_{HH(C)}$ = 7.1 Hz, 1H, Ta*H*$_A$), 8.17 (AMNXYZ, $J_{HP(C)}$ = 61.9 Hz, $J_{HP(A)}$ = 24.1 Hz, $J_{HP(B)}$ = 16.4 Hz, $^2J_{HH(C)}$ = 9.3 Hz, $^2J_{HH(A)}$ = 7.1 Hz, 1H, Ta*H*$_B$), 7.98 and 8.03 (m, 4H total, PPh *o-H*), 9.87 (AMNOXYZ, $J_{HP(B)}$ = 60.2 Hz, $J_{HP(A)}$ = 37.0 Hz, $J_{HP(C)}$ = 9 Hz, $^2J_{HH(B)}$ = 9.3 Hz, $^2J_{HH(A)}$ = 7.1 Hz, $^4J_{HH}$ = 1.4 Hz, 1H, Ta*H*$_C$). ^{31}P{^{1}H}NMR (C₆D₆, 30 °C): δ −21.5 (dd,$^2J_{PP}$ = 31.7, $^2J_{PP}$ = 78.2, Ta*P*Me₃, P$_A$), 20.2 (dd, $^2J_{PP}$ = 31.7, $^2J_{PP}$ = 86.6, [P₂N₂] ligand P$_B$), 37.2 (dd, $^2J_{PP}$ = 86.6, $^2J_{PP}$ = 78.2, [P₂N₂] ligand P$_C$). Anal. Calcd for $C_{27}H_{54}N_2P_3Si_4Ta$: C, 40.90; H, 6.86; N, 3.54. Found: C, 41.03; H, 6.80; N, 3.39.

Synthesis of [P₂N₂]Ta(C₂H₄)Et (1). A stirred red solution of [P₂N₂]-TaH₃(PMe₃) (1.3 g, 1.64 mmol) in 20 mL of hexanes was sealed in a glass vessel equipped with a Teflon valve under an atmosphere of ethylene. After 5 min the gases were evacuated and the vessel was again charged with ethylene. This was repeated and the light orange solution was allowed to stir for 6 h. The gases were evacuated again, and the remaining liquid was transferred to an Erlenmeyer flask in a glovebox. Over 30 min a microcrystalline pale orange solid precipitated from solution. The solid was collected by filtration and dried in vacuo, producing [P₂N₂]Ta(C₂H₄)Et in 95% yield. X-ray quality single crystals were obtained by slow evaporation of a benzene and hexamethyldisiloxane solution. The species [P₂N₂]Ta(C₂H₄)Et is soluble in aromatic solvents but insoluble in hexanes. ^{1}H NMR (C₆D₆, 25 °C, 500 MHz): δ −1.27 ($A_2M_3X_2$, $^3J_{HH}$ = 7.8 Hz, $^3J_{HP}$ = 3.1 Hz, 2H, TaC*H*₂CH₃), −0.51($A_3M_2X_2$, $^3J_{HH}$ = 7.8 Hz, J_{HP} = 4.4 Hz, 3H, TaCH₂C*H*₃), 0.13, 0.23, 0.37, and 0.51 (s, 24H total, SiC*H*₃), 0.55 and 1.47 (m, 4H total, Ta(C₂*H*₄), 1.34, 1.41, 1.70, and 1.70 (AMX, 8H total, C*H*₂ ring), 7.07 (m, 2H, *p-H*), 7.19 (m, 4H, *m-H*), 7.66 (m, 4H, *o-H*). ^{31}P NMR (C₆D₆, 25 °C): δ 24.0 (s). ^{13}C NMR (C₆D₆, 25 °C, 125.76 MHz): δ 5.4 (vt, J_{PC} = 3.2 Hz, Si*C*H₃), 5.8 (vt, J_{PC} = 1.6 Hz, Si*C*H₃), 6.0 (vt, J_{PC} = 1.9 Hz, Si*C*H₃), 6.2 (t, J_{PC} = 4.5 Hz, TaCH₂*C*H₃), 7.0 (vt, J_{PC} = 3.2 Hz, Si*C*H₃), 20.4 and 21.2 (s, *C*H₂ ring), 45.0 (vt, J_{PC} = 4.8 Hz, Ta(*C*₂H₄)), 69.9 (t, J_{PC} = 9.0 Hz, Ta*C*H₂CH₃), 128.6 (vt, J_{PC}= 4.3 Hz, *m-C*), 129.2 (s, *p-C*), 131.0 (vt, J_{PC} = 4.8 Hz, *o-C*), 140.9 (dd, J_{PC} =15.3, 16.2 Hz, *ipso-C*). Anal. Calcd for $C_{28}H_{51}N_2P_2Si_4Ta$: C, 43.62; H, 6.67; N, 3.63. Found: C, 43.93; H, 6.79; N, 3.54.

X-ray Crystallographic Analysis of 1. Crystallographic data for **1** appear in Table 1. The final unit-cell parameters were obtained by least-squares methods on the setting angles for 21854 reflections with 2θ = 4.0−60.1°. The data were processed and corrected for Lorentz and polarization effects. The structure of **1** was solved by heavy-atom Patterson methods and expanded using Fourier techniques. The ethylene and ethyl hydrogen atoms were refined isotropically, and the remaining hydrogen atoms were fixed in calculated positions with C−H = 0.98 Å. Atomic coordinates, anisotropic thermal parameters, complete bond lengths and bond angles, torsion angles, intermolecular contacts, and least-squares planes are included as Supporting Information.

Reaction of [P₂N₂]Ta(C₂H₄)Et (1) with C₂D₄. A solution of [P₂N₂]-Ta(C₂H₄)Et (40 mg, 0.052 mmol) in 1 mL of d_8-toluene in a NMR tube was placed under 1 atm of C₂D₄ then frozen in liquid N₂ and sealed. A ^{1}H NMR spectrum was obtained immediately after thawing. ^{1}H NMR spectrum of selected peaks (C₆D₆, 295 K, 500 MHz): δ −1.52 (br m, [P₂N₂]Ta(C₂(H/D)₄)(C*H*(D)Me)), −1.28 (m, [P₂N₂]Ta(C₂(H/D)₄)-(C*H*₂Me)), −0.75 (br m, [P₂N₂]Ta(C₂(H/D)₄)(CH₂C*H*(D)₂)), −0.64 (br m, [P₂N₂]Ta(C₂(H/D)₄)(CH₂C*H*₂(D)), −0.52 (br m, [P₂N₂]Ta(C₂(H/D)₄)-(CH₂C*H*₃).

Variable-Temperature ^{1}H NMR Study of [P₂N₂]Ta(C₂H₄)Et (1). A solution of [P₂N₂]Ta(C₂H₄)Et (20 mg, 0.026 mmol) in 1 mL of d_8-toluene was sealed under vacuum in a NMR tube. ^{1}H NMR (C₆D₆, 299.9 K, 500 MHz): δ −1.33 (m, 2H, TaC*H*₂CH₃), −0.58 (m, TaCH₂C*H*₃), 0.11, 0.22, 0.34, and 0.49 (s, 24H total, SiC*H*₃), 0.44 and 1.38 (m, 4H total, Ta(C₂*H*₄), 1.32, 1.38, 1.68, 1.68 (AMX, 8H total, C*H*₂ ring), 6.98−7.63 ppm (aromatic region). ^{1}H NMR (C₆D₆, 279.9 K, 500 MHz): δ −1.31 (m, 2H, TaC*H*₂CH₃), −0.68 (m, TaCH₂C*H*₃), 0.14, 0.24, 0.36, and 0.50 (s, 24H total, SiC*H*₃), 0.33 and 1.36 (m, 4H total, Ta(C₂*H*₄), 1.30, 1.36, 1.66, and 1.67 (AMX, 8H total, C*H*₂ ring), 6.98−7.63 ppm (aromatic region). ^{1}H NMR (C₆D₆, 259.9 K, 500 MHz): δ −1.28 (m, 2H, TaC*H*₂CH₃), −0.79 (m, TaCH₂C*H*₃), 0.17, 0.26, 0.36, and 0.50 (s, 24H total, SiC*H*₃), 0.27 and 1.34 (m, 4H total, Ta(C₂*H*₄), 1.27, 1.34, 1.64, and 1.65 (AMX, 8H total, C*H*₂ ring), 6.98−7.63 ppm (aromatic region). ^{1}H NMR (C₆D₆, 239.9 K, 500 MHz): δ −1.26 (m, 2H, TaC*H*₂CH₃), −0.87 (m, TaCH₂C*H*₃), 0.20, 0.28, 0.38, and 0.53 (s, 24H total, SiC*H*₃), 0.21 and 1.34 (m, 4H total, Ta(C₂*H*₄), 1.24, 1.34, 1.64, and 1.64 (AMX, 8H total, C*H*₂ ring), 6.98−7.63 ppm (aromatic region). ^{1}H NMR (C₆D₆, 200.0 K, 500 MHz): δ −1.21 (m, 2H, TaC*H*₂CH₃), −1.03 (m, TaCH₂C*H*₃), 0.28, 0.33, 0.41, and 0.59 (s, 24H total, SiC*H*₃), 0.11 and 1.34 (m, 4H total, Ta(C₂*H*₄), 1.19, 1.34, 1.61, and 1.61 (AMX, 8H total, C*H*₂ ring), 6.98−7.63 ppm (aromatic region). ^{1}H NMR (C₆D₆, 183.0 K, 500 MHz): δ −1.17 (m, 2H, TaC*H*₂-

CH_3), −1.10 (m, $TaCH_2CH_3$), 0.32, 0.37, 0.43, and 0.62 (s, 24H total, $SiCH_3$), 0.08 and 1.35 (m, 4H total, $Ta(C_2H_4)$, 1.16, 1.29, 1.62, and 1.62 (AMX, 8H total, CH_2 ring), 6.98−7.63 ppm (aromatic region).

Variable-Temperature Isotopic Perturbation of Resonance Experiment. To a sample of $[P_2N_2]Ta(C_2H_4)Et$ (30 mg, 0.0389 mmol) in benzene was condensed C_2D_4 gas (6.4 mL, 0.26 mmol) to produce a mixture of isotopomers containing ∼75% deuterium labels in the ethyl group. After reacting for several months, this solution was evaporated to dryness, dissolved in d_8-toluene, and sealed in a NMR tube. The calculated relative intensities of the NMR signals for the various possible isotopomers with 75% deuterium labels are as follows: α-position CH_2CH_3, 0.2; $CHDCH_3$, 0.6; CD_2CH_3, 0.0; CH_2CH_2D, 1.8; $CHDCH_2D$, 5.3; CD_2CH_2D, 0.0; CH_2CHD_2, 5.3; $CHDCHD_2$, 15.8; CD_2CHD_2, 0.0; CH_2CD_3, 5.3; $CHDCD_3$, 15.8; CD_2CD_3, 0.0. β-position CH_2CH_3, 0.3; $CHDCH_3$, 1.8; CD_2CH_3, 2.6; CH_2CH_2D, 1.8; $CHDCH_2D$, 10.5; CD_2CH_2D, 15.8; CH_2CHD_2, 2.6; $CHDCHD_2$, 15.8; CD_2CHD_2, 23.7; CH_2CD_3, 0.0; $CHDCD_3$, 0.0; CD_2CD_3, 0.0. ^{1}H NMR, ethyl region (C_7H_8, 295 K) −0.65 (br overlapping, $CHDCH_3$ and CD_2CH_3), −0.75 (br overlapping, $CHDHCH_2D$ and CD_2CH_2D), −0.81 (br, $CHDCHD_2$), −0.85 (br, CD_2CHD_2), −1.37 (br overlapping, CH_2CHD_2 and CH_2CD_3), −1.57 (overlapping, $CHDCHD_2$ and $CHDCD_3$).^{1}H NMR, ethyl region (C_7H_8, 274.6 K) −0.81 (br overlapping, $CHDCH_3$ and CD_2CH_3), −0.85 (br, $CHDCH_2D$), −0.90 (br, CD_2CH_2D), −0.96 (br, $CHDCHD_2$), −1.00 (br, CD_2CHD_2), −1.34 (br overlapping, CH_2CHD_2 and CH_2CD_3), −1.53 (overlapping, $CHDCHD_2$ and $CHDCD_3$). ^{1}H NMR, ethyl region (C_7H_8, 254.6 K) −0.90 (br, $CHDCH_3$), −0.95 (br, CD_2CH_3), −1.00 (br, $CHDCH_2D$), −1.05 (br, CD_2CH_2D), −1.10 (br, $CHDCHD_2$), −1.16 (br, CD_2CHD_2), −1.31 (overlapping multiplets, CH_2CHD_2 and CH_2CD_3), −1.49 (overlapping, $CHDCHD_2$ and $CHDCD_3$). ^{1}H NMR, ethyl region (C_7H_8, 234.6 K) −0.99 (br, $CHDCH_3$), −1.05 (br, CD_2CH_3), −1.10 (br, $CHDCH_2D$), −1.17 (br, CD_2CH_2D), −1.19 (br, $CHDCHD_2$), −1.28 (br, CD_2CHD_2), −1.28 (overlapping, CH_2CHD_2 and CH_2CD_3), −1.46 (overlapping, $CHDCHD_2$ and $CHDCD_3$).

EXSY Spectrum of $[P_2N_2]Ta(C_2H_4)Et$ (1). ^{1}H EXSY (C_6D_6, τ = 0.4 s, 300 K) cross-signals δ −0.51, 0.55 and −0.51, 1.47 ($TaCH_2CH_3$, $Ta(C_2H_4)$); −1.28, 0.55 and −1.28, 1.47 ($TaCH_2CH_3$, $Ta(C_2H_4)$); 0.13, 0.37 and 0.23, 0.51 (ligand $SiCH_3$, ligand $SiCH_3$).

Acknowledgment. We gratefully acknowledge both the NSERC of Canada and the Petroleum Research Fund, administered by the American Chemical Society, for funding in the form of research grants. Financial support was also provided by the NSERC of Canada in the form of a postgraduate scholarship for S. A. Johnson, as well as the University of British Columbia in the form of a University Graduate Fellowship.

Supporting Information Available: Full experimental details, tables of X-ray parameters, fractional coordinates and thermal parameters, bond lengths, bond angles, and torsion angles, and an ORTEP diagram for compound **1** (PDF). This material is available free of charge via the Internet at http://pubs.acs.org.

JA0021621